Biointerface Research in Applied Chemistry
Open-Access Journal (ISSN: 2069-5837)

Article
Volume 13, Issue 6, 2023, 518
https://doi.org/10.33263/BRIAC136.518

Electrochemical Profile of TiO_2/Ti-Coated Nickel Slag Photoelectrode Prepared by Electrodeposition Method

Ismaun Ismaun [1], Zul Arham [1,*], Irwan Irwan [2]

[1] Department of Mathematics and Natural Sciences, Institute Agama Islam Negeri (IAIN), Kendari 93563–Southeast Sulawesi, Indonesia; ismaun85.iainkdi@gmail.com (I.I.); arhamzul88@yahoo.com (Z.A.);
[2] Department of Pharmacy, Faculty of Sciences and Technology, Institut Teknologi dan Kesehatan Avicenna, Kendari 93117, Southeast Sulawesi, Indonesia; nazrilirwan16@gmail.com (I.I.);
* Correspondence: arhamzul88@yahoo.com (Z.A.);

Scopus Author ID 57195056274
Received: 1.10.2022; Accepted: 18.11.2022; Published: 4.02.2023

Abstract: Herein, slag-TiO_2/Ti photoelectrode was prepared by deposition technique using a Ti plate as a template. The influence of slag doping on TiO_2/Ti photoelectrode electrochemical performance was investigated. Previously, TiO_2/Ti photoelectrode was synthesized by an anodizing method in an electrolyte solution containing glycerol, DI water, and NH_4F. This study also varied the measurement of potential difference and deposition time photoelectrode. In addition, there has unique excellence, such as high surface area and stability. The electro-chemical studies of slag-TiO_2/Ti photoelectrode were determined using Linear Sweep Voltammetry (LSV) technique in $K_3[Fe(CN)_6]$ electrolyte solution. We found the slag composition with various mineral dominant contents such as Fe_2O_3, Al_2O_3, MgO, and SiO_2, respectively 10.37%, 2.98%, 21.96%, and 38.71%. The results exhibit that the modified slag-TiO_2/Ti photoelectrode with a potential difference of 2.0 Volt and a deposition time of 15 minutes presents higher electrochemical performance and good stability than other photoelectrodes.

Keywords: Nickel slag; TiO_2/Ti photoelectrode; electrodeposition method; linear sweep voltammetry.

1. Introduction

The surface phenomenon of TiO_2 semiconductor material, which can be applied as a photocatalytic material in decomposing organic pollutants, has attracted the attention of researchers around the world in recent years. The surface of TiO_2 can absorb UV-Vis light and produce a hole (h) which is a strong oxidizing agent, so it's very effective in degrading organic pollutants that are difficult to degrade by methods that have been developed previously [1,2]. In addition, other advantages of TiO_2 are environmentally friendly, non-toxic, and high photocatalytic activity [3,4].

Several obstacles in applying TiO_2 as a photocatalytic material, such as catalyst recovery, are difficult to carry out, thus triggering new pollution. Moreover, the electron-hole pair recombination that occurs is very fast, causing inefficient degradation. On the other hand, TiO_2 can only absorb UV light around 4-6% in sunlight, prompting the need for surface modification of TiO_2 [5,6]. Doping methods use non-metallic elements (such as N, B, C, F), transition metals (such as Fe, Ni, Cu, Zn, Mn, Cr), and lanthanide metals, showing increased photocatalytic activity of TiO_2 under UV irradiation [7]. Its performance successfully extended the working area of TiO_2 to Visible light, thus allowing for a wider range of applications using

direct sunlight [8–12]. In addition to the doping method, the working electrode-based photoelectrocatalytic method was also reported to improve the photocatalytic activity of TiO_2, where this method can reduce the rate of electron-hole pair recombination and provide better degradation results [13,14].

Seeing the promising prospect of the TiO_2 semiconductor, it became a passion for modifiying the surface of this material. So in this research, TiO_2/Ti surface doping will be carried out through electrochemical anodizing using Pomalaa nickel processing slag waste as the metal element. Based on the literature study, in addition to Ni, Slag waste also contains many other transition elements such as Cu, Zn, Fe, and Co. Furthermore, it also contains metals such as In, Ge, and Al [15,16]. The existence of these elements can be a leverage for the success of this research. Moreover, using Pomalaa nickel processing slag as a doping material is a breakthrough. It can be used as an alternative step in processing nickel slag waste which is reported to increase yearly.

2. Materials and Methods

2.1. Materials.

The materials used in this study were titanium plate (0.5 mm thick and 99% pure), ammonium fluoride (NH_4F), ethanol (C_2H_5OH), distilled water, potassium ferricyanide $K_3[Fe(CN)_6]$, methylene blue (MB) dye was purchased from Sigma–Aldrich (M). Especially nickel slag obtained from PT. Antam Pomalaa-Koalaka, Southeast Sulawesi-Indonesia.

2.2. Preparation and characterization of nickel slag.

Slag samples were obtained from the Pomalaa Nickel Processing Slag waste reservoir. It was ground mechanically using a disk mill. Hereafter, the slag was sifted using a 100 µm size. Finally, the slag was characterized by XRF to notice the oxide composition.

2.3. Formation of slag-TiO_2/Ti by electrodeposition method.

The prepared Ti plate was inserted into a probe containing an electrolyte solution of an 87% glycerol solution and distilled water with a volume ratio of 24:1 and 0.27 M NH4F. Ti plate was cut with lengths of 4 cm and width of 0.5 cm, respectively. Anodizing was done for 4 hours by placing the Ti plate as the anode and the Cu plate as the cathode using a potential difference of 25 V, which was connected to the power supply. The electrodes formed were then doped with a slag solution using the electrodeposition method to produce slag-TiO_2/Ti electrodes. Finally, the slag-TiO_2/Ti electrode was calcined for three h at 500 °C.

2.4. The electrochemical activity of the photoelectrode.

The electrochemical activity test of the electrode was observed using the Linear Sweep Voltammetry (LSV) technique in 0.1 M $K_3[Fe(CN)_6]$ electrolyte solution using a 3-electrode system. The electrodes used include slag-TiO_2/Ti photoelectrode as a working electrode, platinum (Pt) wire as a counter electrode, and Ag/AgCl electrode as a comparison electrode. Measurements were made from a potential range of -1V - 1 V with a scan rate of 0.1 V/s.

3. Results and Discussion

3.1. Electrodeposition of slag-TiO_2/Ti.

The electrodeposition process increases the activity of the TiO_2 photocatalyst by adding dopant slag to the TiO_2 crystal lattice. The potential difference varies, including 1 Volt, 1.5 Volt, and 2 Volt with a time of 10 minutes. The selection of a temperature of 500 °C during the calcination process aims to glue the Slag-TiO_2/Ti layer to make it stronger so that the bonding force between the thin layer and the TiO_2 formed by the Ti plate layer is getting better. In addition, it removes the remaining water solvent and forms TiO_2 crystals in the anatase phase [17,18]. Visually the results obtained in the electrodeposition process are shown in Figure 1.

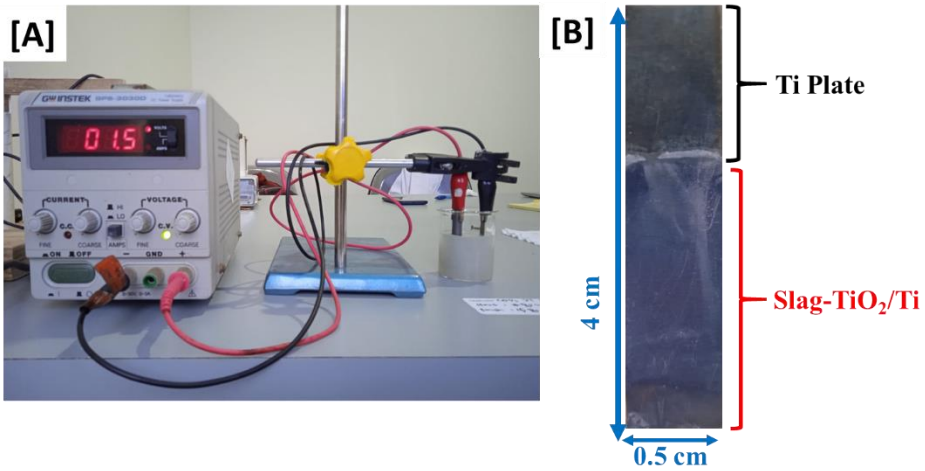

Figure 1. (A) Slag-TiO_2/Ti electrodeposition process and **(B)** slag-TiO_2/Ti photoelectrode

3.2. Characterization of slag composition and morphology of TiO_2/Ti.

The slag sample used was obtained from PT. Antam Pomalaa-Kolaka. The slag, still in the form of lumps, was washed using clean water to remove impurities such as soil and grass. The prepared slag samples were then analyzed using XRF to see the content of the elements and activated to remove the impurities. The results of XRF characterization on the slag sample showed the presence of dominant oxide compounds such as Fe_2O_3, Al_2O_3, MgO, and SiO_2, respectively 10.37%, 2.98%, 21.96%, and 38.71%. The rest were compounded minor compounds such as Ni, Co, TiO_2, and Zn, which have a small percentage (Table 1).

Table 1. Characterization of XRF slag before activation.

No.	Element	Composition (%)
1.	Ni	0.06
2.	Fe	7.25
3.	Co	0.0002
4.	MgO	21.96
5.	SiO_2	38.71
6.	Si	18.09
7.	Fe_2O_3	10.37
8.	Cr_2O_3	1.17
9.	Al_2O_3	2.98
10.	CaO	1.14
11.	MnO	0.35
12.	TiO_2	0.07
13.	K_2O	<0.01

No.	Element	Composition (%)
14.	Na_2O	0.001
15.	P_2O_5	0.001
16.	SO_3	0.09
Total		**100 %**

SEM was used to determine the surface structure and morphology of the TiO_2/Ti photoelectrode prepared. The surface morphology of the anodized TiO_2/Ti electrode with a potential difference of 25 V for 4 hours, calcined at a temperature of 500 °C, was shown in Figure 2. The results show the formation of TiO_2 nanopores on the surface of the Ti plate [19,20]. The presence of glycerol in the anodizing process greatly affects the resulting oxide layer. Low water content in glycerol will form an oxide layer with good homogeneity. The high viscosity of the glycerol solution allows the movement of the electrolyte ions (F- ions) in the solution to be more limited so that the oxide layer formed has good regularity [21,22]. In addition, the presence of NH_4F solution in the anodizing process will result in the formation of a tube template on the photoelectrode.

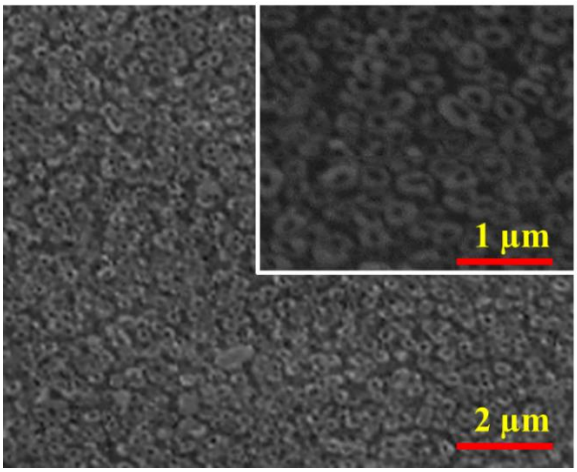

Figure 2. Surface morphology of TiO_2/Ti photoelectrode.

3.3 Electrochemical test of slag-TiO_2/Ti photoelectrodes

An electrochemical test of the electrode was observed using the Linear Sweep Voltammetry (LSV) method in 0.1 M [$K_3(FeCN_6)$] electrolyte solution using a 3-electrode portable potentiostat system [23,24]. Slag-TiO_2/Ti photoelectrode as the working electrode, platinum wire (Pt) as an auxiliary electrode, and Ag/AgCl electrode as the comparison electrode. An electrode test was carried out to see the effect of slag dopants on the photoelectrolysis system. The results of the LSV test are shown in Figure 3.

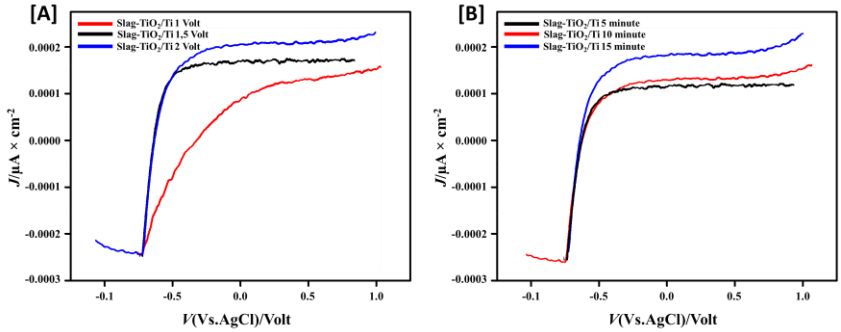

Figure 3. Amperogram of slag-TiO_2/Ti photoelectrodes; **(A)** variation of potential difference, and **(B)** variation of deposition time.

Based on Figure 3A, it can be seen that the potential difference applied to the slag-TiO_2/Ti working electrode in the photoelectrocatalyst system causes the formation of a positive electric field due to a decrease in the fermi energy level. The resulting electrons are transferred to the Pt auxiliary electrode via an external circuit. On the other hand, the holes produced in the valence band will be brought to the TiO_2 surface to attack the material in contact with the catalyst surface to initiate the oxidation reaction of organic compounds. Therefore, the potential difference increases the e^-/h^+ separation and the rate of photohole capture by the target compound, which will increase the efficiency of photodegradation on the electrode surface.

The deposition time affects the testing process because the deposition time can increase the sensitivity and lower the detection limit. The pre-concentration stage can have an influence on the measurement of the analyte current at the slag-TiO_2/Ti working electrode. Based on Figure 3B, it can be seen that with increasing deposition time, the resulting current is greater. This is because, with increasing deposition time, the opportunity to reduce the slag solution in the solution will be greater so that more ions will be trapped on the surface of the photoelectrode [25–27]. These ions will help the degradation process of analyte compounds.

3.4 Determination of Scan Rate

A study of the effect scan rate was carried out using the LSV technique in $K_3[Fe(CN)_6]$ electrolyte solution. Measurements were made on photoelectrodes with a potential difference of 1 Volt, 1.5 Volt, and 2 Volt. The electron transfer that occurs at the slag-TiO_2/Ti photoelectrode was affected by the scan rate. Variations of scan rate used in this research include 0.05; 0.1; 0.2, and 0.5 V/s. Based on the results in Figure 4, it can be seen that the photoelectrode with a potential of 2 Volts shows higher electrochemical performance and good stability than other photoelectrodes.

Moreover, the optimum scan rate was shown at a scan rate of 0.5 V/s. This phenomenon was caused by slag in the TiO_2/Ti electrode, which can help the electron transfer process so that the redox reaction rate becomes faster at the electrode surface [28,29]. A larger scan rate would be caused the time needed to reach equilibrium to be faster as well [30]. Conversely, a lower scan rate will result in a thinner diffusion layer.

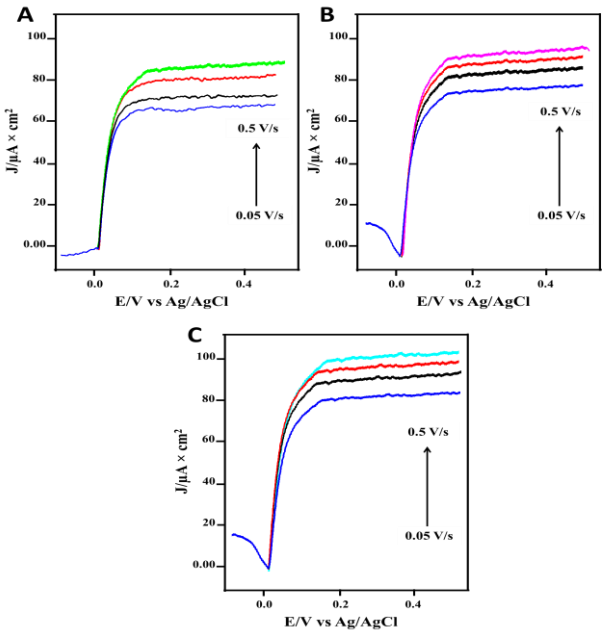

Figure 4. Potential difference variation; **(A)** 1 Volt, **(B)** 1.5 Volt, and **(C)** 2 Volt.

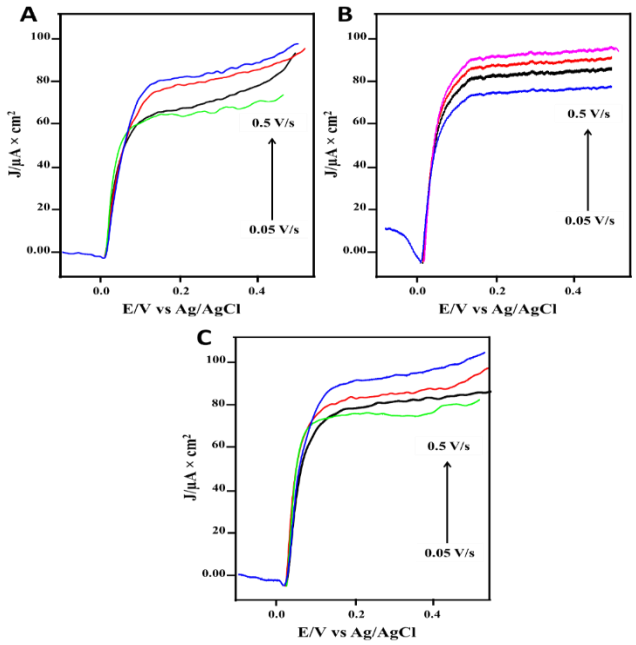

Figure 5. Variation of deposition time; **(A)** 5 minute, **(B)** 10 minutes, and **(C)** 15 minute

The scan rate was determined by varying the scan rate, namely 0.05 V/s, 0.1 V/s, 0.2 V/s, and 0.5 V/s, with deposition times of 5 minutes, 10 minutes, and 15 minutes. Measurements were made with a potential range of 1 V-1 V in $K_3[Fe(CN)_6]$ electrolyte solution [31]. It can be seen that (Figure 5) the resulting voltammogram increases as the scan rate increases. Increasing the scan rate would be caused a high current of the analyte redox reaction [32]. The highest peak current was generated at the photoelectrode with a deposition time variation of 10 minutes. This phenomenon was caused by a high scan rate. The diffusion layer formed will be thin so that the transfer of electrons around the surface of the working electrode takes place properly [18,29,33].

4. Conclusions

In summary, the electrodeposition method successfully synthesized the slag-TiO_2/Ti photoelectrode. In short, TiO_2/Ti photoelectrode was synthesized by the anodizing method in an electrolyte solution containing glycerol, DI water, and NH_4F. This study also varied the measurement of potential difference and deposition time electrode. XRF analyses further confirmed the presence of dominant mineral contents such as Fe_2O_3, Al_2O_3, MgO, and SiO_2, respectively 10.37%, 2.98%, 21.96%, and 38.71%. The experimental results LSV exhibited that slag-TiO_2/Ti photoelectrode with a potential difference of 2.0 Volt and deposition time of 15 minutes presents higher electrochemical performance and good stability compared with another photoelectrode.

Funding

This research was funded by the Institute for Research and Community Service IAIN Kendari for research in 2022.

Acknowledgments

The authors acknowledge the assistance financial and laboratory facilities support from the Department of Mathematics and Natural Sciences, Institute Agama Islam Negeri (IAIN) Kendari, Indonesia.

Conflicts of Interest

We Declare conflicts that this article has no conflict of interest.

References

1. Palomares-Reyna, D.; Carrera-Crespo, J.E.; Sosa-Rodríguez, F.S.; García-Pérez, U.M.; Fuentes-Camargo, I.; Lartundo-Rojas, L.; Vazquez-Arenas, J. Photo-electrochemical and ozonation process to degrade ciprofloxacin in synthetic municipal wastewater, using C, N-codoped TiO2 with high visible-light absorption. *Journal of Environmental Chemical Engineering* **2022,** *10*, 107380, https://doi.org/10.1016/j.jece.2022.107380.
2. Ren, Y.; Xing, S.; Wang, J.; Liang, Y.; Zhao, D.; Wang, H.; Wang, N.; Jiang, W.; Wu, S.; Liu, S. Weak-light-driven Ag–TiO2 photocatalyst and bactericide prepared by coprecipitation with effective Ag doping and deposition. *Optical Materials* **2022,** *124*, 111993, https://doi.org/10.1016/j.optmat.2022.111993.
3. Abd El-Kader, M.F.H.; Elabbasy, M.T.; Adeboye, A.A.; Zeariya, M.G.M.; Menazea, A.A. Morphological, structural and antibacterial behavior of eco-friendly of ZnO/TiO2 nanocomposite synthesized via Hibiscus rosa-sinensis extract. *Journal of materials research and technology* **2021,** *15*, 2213–2220, https://doi.org/10.1016/j.jmrt.2021.09.048.
4. Arora, I.; Chawla, H.; Chandra, A.; Sagadevan, S.; Garg, S. Advances in the strategies for enhancing the photocatalytic activity of TiO2: Conversion from UV-light active to visible-light active photocatalyst. *Inorganic Chemistry Communications* **2022,** 109700, https://doi.org/10.1016/j.inoche.2022.109700.
5. Wang, Q.; Xiao, L.; Liu, X.; Sun, X.; Wang, J.; Du, H. Special Z-scheme Cu3P/TiO2 hetero-junction for efficient photocatalytic hydrogen evolution from water. *Journal of Alloys and Compounds* **2022,** *894*, 162331, https://doi.org/10.1016/j.jallcom.2021.162331.
6. Qutub, N.; Singh, P.; Sabir, S.; Sagadevan, S.; Oh, W.-C. Enhanced photocatalytic degradation of Acid Blue dye using CdS/TiO2 nanocomposite. *Scientific Reports* **2022,** *12*, 1–18, https://www.nature.com/articles/s41598-022-09479-0.
7. Arham, Z.; Kurniawan, K.; Ismaun, I. Synthesis of TiO2 Photoelectrode Nanostructures for Sensing and Removing Textile Compounds Rhodamine B. *Biointerface Research in Applied Chemistry* **2021,** https://biointerfaceresearch.com/wp-content/uploads/2021/10/20695837124.54795485.pdf.
8. Liu, H.; Xu, G.; Wang, J.; Lv, J.; Zheng, Z.; Wu, Y. Photoelectrochemical properties of TiO2 nanotube arrays modified with BiOCl nanosheets. *Electrochimica Acta* **2014,** *130*, 213–221, https://doi.org/10.1016/j.electacta.2014.03.005.
9. Gross, P.A.; Pronkin, S.N.; Cottineau, T.; Keller, N.; Keller, V.; Savinova, E.R. Effect of deposition of Ag nanoparticles on photoelectrocatalytic activity of vertically aligned TiO2 nanotubes. *Catalysis today* **2012,** *189*, 93–100, https://doi.org/10.1016/j.cattod.2012.03.054.
10. Zhang, M.; Yuan, S.; Wang, Z.; Zhao, Y.; Shi, L. Photoelectrocatalytic properties of Cu2+-doped TiO2 film under visible light. *Applied Catalysis B: Environmental* **2013,** *134*, 185–192, https://doi.org/10.1016/j.apcatb.2013.01.024.
11. Rashad, M.M.; Elsayed, E.M.; Al-Kotb, M.S.; Shalan, A.E. The structural, optical, magnetic and photocatalytic properties of transition metal ions doped TiO2 nanoparticles. *Journal of Alloys and Compounds* **2013,** *581*, 71–78, https://doi.org/10.1016/j.jallcom.2013.07.041.
12. Wang, F.; Yan, X.; Xu, M.; Li, S.; Fang, W. Electrochemical performance and electroreduction of maleic acid on Ce-doped nano-TiO2 film electrode. *Electrochimica Acta* **2013,** *97*, 253–258, https://doi.org/10.1016/j.electacta.2013.03.009.
13. Sharma, H.K.; Sharma, S.K.; Vemula, K.; Koirala, A.R.; Yadav, H.M.; Singh, B.P. CNT facilitated interfacial charge transfer of TiO2 nanocomposite for controlling the electron-hole recombination. *Solid State Sciences* **2021,** *112*, 106492, https://doi.org/10.1016/j.solidstatesciences.2020.106492.
14. Chakhtouna, H.; Benzeid, H.; Zari, N.; Bouhfid, R. Recent progress on Ag/TiO2 photocatalysts:

photocatalytic and bactericidal behaviors. *Environmental Science and Pollution Research* **2021,** *28*, 44638–44666, https://link.springer.com/article/10.1007/s11356-021-14996-y.
15. Jian, P.A.N.; Zheng, G.; Zhu, D.; Zhou, X. Utilization of nickel slag using selective reduction followed by magnetic separation. *Transactions of Nonferrous Metals Society of China* **2013,** *23*, 3421–3427, https://doi.org/10.1016/S1003-6326(13)62883-6.
16. Ahmed, I.M.; Nayl, A.A.; Daoud, J.A. Leaching and recovery of zinc and copper from brass slag by sulfuric acid. *Journal of Saudi Chemical Society* **2016,** *20*, S280–S285, https://doi.org/10.1016/j.jscs.2012.11.003.
17. Maulidiyah; Azis, T.; Nurwahidah, A.T.; Wibowo, D.; Nurdin, M. Photoelectrocatalyst of Fe co-doped N-TiO2/Ti nanotubes: Pesticide degradation of thiamethoxam under UV–visible lights. *Environmental Nanotechnology, Monitoring and Management* **2017,** *8*, 103–111 https://doi.org/10.1016/j.enmm.2017.06.002.
18. Nurdin, M.; Maulidiyah, M.; Muzakkar, M.Z.; Umar, A.A. High performance cypermethrin pesticide detection using anatase TiO2-carbon paste nanocomposites electrode. *Microchemical Journal* **2019,** *145*, 756–761, https://doi.org/10.1016/j.microc.2018.11.050.
19. Nurdin, M.; Muzakkar, M.Z.; Maulidiyah, M.; Trisna, T.; Arham, Z.; La Salim, O.A.; Irwan, I.; Umar, A.A. High-Performance COD Detection of Organic Compound Pollutants using Sulfurized-TiO2/Ti Nanotube Array Photoelectrocatalyst. *Electrocatalysis* **2022,** 1–10, https://link.springer.com/article/10.1007/s12678-022-00746-2.
20. Nurdin, M.; Wibowo, D.; Azis, T.; Safitri, R.A.; Maulidiyah, M.; Mahmud, A.; Mustapa, F.; Ruslan, R.; Salim, A.; Ode, L. Photoelectrocatalysis Response with Synthetic Mn–N–TiO2/Ti Electrode for Removal of Rhodamine B Dye. *Surface Engineering and Applied Electrochemistry* **2022,** *58*, 125–134, https://link.springer.com/article/10.3103/S1068375522020077.
21. Muzakkar, M.Z.; Umar, A.A.; Ilham, I.; Saputra, Z.; Zulfikar, L.; Maulidiyah, M.; Wibowo, D.; Ruslan, R.; Nurdin, M. Chalcogenide material as high photoelectrochemical performance Se doped TiO2/Ti electrode: Its application for Rhodamine B degradation. *Journal of Physics: Conference Series* **2019,** *1242*, https://doi.org/10.1088/1742-6596/1242/1/012016.
22. Nurdin, M.; Azis, T.; Maulidiyah, M.; Aladin, A.; Hafid, N.A.; Salim, L.O.A.; Wibowo, D. Photocurrent Responses of Metanil Yellow and Remazol Red B Organic Dyes by Using TiO2/Ti Electrode. *IOP Conference Series: Materials Science and Engineering* **2018,** *367*, https://doi.org/10.1088/1757-899X/367/1/012048.
23. Wibowo, D.; Indah Sari, W.O.S.; Said, A.; Mustapa, F.; Susianti, B.; Maulidiyah, M.; Nurdin, M. Electrochemical-Sensor Behavior for Determination of Low Urea Concentration using Graphite-TiO2 Composites Immobilized in a Glass Tube. *Analytical and Bioanalytical Electrochemistry* **2022,** *14*, 385–401, http://www.abechem.com/article_252040.html
24. Wibowo, D.; Malik, R.H.A.; Mustapa, F.; Nakai, T.; Maulidiyah, M.; Nurdin, M. Highly Synergistic Sensor of Graphene Electrode Functionalized with Rutile TiO2 Microstructures to Detect L-Tryptophan Compound. *Journal of Oleo Science* **2022,** *71*, 759–770, https://doi.org/10.5650/jos.ess21416.
25. Jang, H.J.; Park, S.J.; Yang, J.H.; Hong, S.-M.; Rhee, C.K.; Sohn, Y. Photocatalytic and electrocatalytic properties of Cu-loaded ZIF-67-derivatized bean sprout-like Co-TiO2/Ti nanostructures. *Nanomaterials* **2021,** *11*, 1904, https://doi.org/10.3390/nano11081904.
26. Mashhadizadeh, M.H.; Azhdeh, A.; Moazami, H.R.; Sheydaei, M. Development of a wireless feeding system for highly effective electro-photocatalytic degradation of organic pollutants from aqueous solutions. *Electrochimica Acta* **2021,** *391*, 138991, https://doi.org/10.1016/j.electacta.2021.138991.
27. Goulart, L.A.; Santos, G.O.S.; Eguiluz, K.I.B.; Salazar-Banda, G.R.; Lanza, M.R. V; Saez, C.; Rodrigo, M.A. Towards a higher photostability of ZnO photo-electrocatalysts in the degradation of organics by using MMO substrates. *Chemosphere* **2021,** *271*, 129451, https://doi.org/10.1016/j.chemosphere.2020.129451.
28. Maulidiyah, M.; Azis, T.; Lindayani, L.; Wibowo, D.; Salim, L.O.A.; Aladin, A.; Nurdin, M. Sol-gel TiO2 carbon paste electrode nanocomposites for electrochemical-assisted sensing of fipronil pesticide. *Journal of Electrochemical Science and Technology* **2019,** *10*, https://doi.org/10.33961/jecst.2019.00178.
29. Nurdin, M.; Dali, N.; Irwan, I.; Maulidiyah, M.; Arham, Z.; Ruslan, R.; Hamzah, B.; Sarjuna, S.; Wibowo, D. Selectivity Determination of Pb2+ Ion Based on TiO2-Ionophores BEK6 as Carbon Paste Electrode Composite. *ANALYTICAL & BIOANALYTICAL ELECTROCHEMISTRY* **2018,** *10*, 1538–1547, https://www.sid.ir/paper/346533/en.
30. Dali, N.; Maulidiyah, M.; Samsiah, S.; Irwan, I.; Salim, L.O.A.; Arham, Z.; Nurdin, M. Modification of Carbon Paste Electrode Using Calyx [6] Arene-TiO2 Nanocomposite for Determination of Cu2+ ion Based

on Cyclic Voltammetry. *Biointerface Research in Applied Chemistry* **2021,** https://biointerfaceresearch.com/wp-content/uploads/2021/08/20695837123.28432851.pdf.

31. Arham, Z.; Kurniawan, K. Electrode modifier performance of TiO2 incorporated carbon quantum dots nanocomposites on Fe (CN) 6 3−/Fe (CN) 6 4− electrochemical system. *Korean Journal of Chemical Engineering* **2022;** *39*, pp. 1333–1338, https://link.springer.com/article/10.1007/s11814-021-0980-4.
32. Nurdin, M.; Maulidiyah, M.; Watoni, A.H.; Armawansa, A.; Salim, L.O.A.; Arham, Z.; Wibowo, D.; Irwan, I.; Umar, A.A. Nanocomposite design of graphene modified TiO2 for electrochemical sensing in phenol detection. *Korean Journal of Chemical Engineering* **2022,** *39*, 209–215, https://link.springer.com/article/10.1007/s11814-021-0938-6.
33. Nurdin, M.; Agusu, L.; Putra, A.A.M.; Maulidiyah, M.; Arham, Z.; Wibowo, D.; Muzakkar, M.Z.; Umar, A.A. Synthesis and electrochemical performance of graphene-TiO 2 -carbon paste nanocomposites electrode in phenol detection. *Journal of Physics and Chemistry of Solids* **2019,** *131*, 104–110 https://doi.org/10.1016/j.jpcs.2019.03.014.